Nonlinear Control of a Buoyancy Driven Airship

Xiaotao . Wu, Claude Moog, L. A. Marquez Martinez

Nonlinear Control of a Buoyancy-Driven Airship

Xiaotao WU Claude H. MOOG L.A. MARQUEZ MARTINEZ and Yueming HU

***Abstract*— The control of a new kind of airship is presented. By restricting its flight to a vertical plane, the mathematical model is reduced. The simplified model is proved to be minimum phase, and a nonlinear controller based on input-output linearization is designed. Since the performance of the controller is significantly impacted by the choice of parameters, simulations of three different pole placement strategies are presented. The nonlinear controller shows better performances than a linear LQR controller when the initial condition is significantly away from the desired equilibrium.**

I. Introduction

Airships attract people's interest again in the recent ten years for their new applications [1], [2], and there is a lot of research on its stability, control, planning and tracking of trajectories [3], [4], [5]. Almost all of these works are based on airships which are driven by propulsors along the hull, and the attitude is controlled by elevators and rudders or vector-propulsors. These mathematical models are all derived from the Gomes model [3].

In this paper, a new kind of airship will be considered, which moves forward by a cyclic change of the net buoyancy of the craft and the position of the ballast. This concept of airship is derived from underwater gliders who replace traditional thrust propulsion by a cyclic change of the net buoyancy and of the position of the centroid [6], which has proved to be efficient in water [7]. The structure of this new kind of airship, the inertial frame $\{G,\ i,\ j,\ k\}$, and the non inertial frame $\{O,\ e_1,\ e_2,\ e_3\}$ are shown in Figure 1. A blower is used to fill an hermetic inner bladder with ambient air, and the valve is used to release the inner air. The ballast can move backward and forward.

The mechanism to operate this kind of airship is as follows. When releasing air from ballonets, the mass of the airship reduces, the lift becomes positive. Accompanying the ballast moves to the tail, the airship gets a positive pitch angle θ. Then it moves upward and forward, see Figure 2. Oppositely, when pumping air into ballonets, the airship's mass increases, the lift decreases and becomes negative. With the ballast moving to the head, the pitch angle θ becomes negative. So it moves downward and forward, see Figure 3.

This work was supported by CSC

X. WU is with Institut de Recherche en Communications et Cybernétique de Nantes, 1 rue de la Noë, 44321, Nantes, France, and South China University of Technology xiaotao.wu@irccyn.ec-nantes.fr

C. H. MOOG is with Institut de Recherche en Communications et Cybernétique de Nantes, claude.moog@irccyn.ec-nantes.fr

L. A. MARQUEZ MARTINEZ is with Institut de Recherche en Communications et Cybernétique de Nantes on leave from CICESE, Ensenada, Mexico, lmarquez@cicese.mx

Y. HU is with South China University of Technology, auymhu@scut.edu.cn

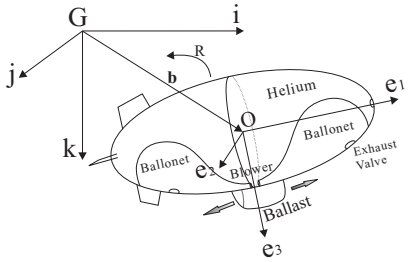

Fig. 1. Structure of Buoyancy-Driven Airship

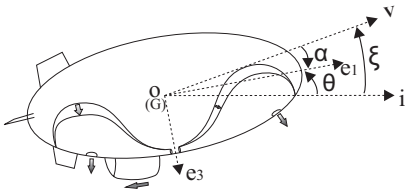

Fig. 2. Ascent of Buoyancy-Driven Airship

If the ballast is moving to the side, then the airship will roll. Due to the coupling of roll and rotation moments, the airship flies to the right or the left [5], [6].

This new kind of airship flies more efficiently than airships with thrusters under some conditions. At present, the only monograph available on buoyancy-driven airship is the doctoral dissertation [5]. This pioneering studies the feasibility and physical model of this kind of airship, and gives a PID control for the system. However, the complete mathematical model of 6DOF is not given, and the control method also needs to be improved. These motivates this work. The complete equations of 6DOF motion can be found in [8], and a linear LQR controller was designed. The model considered herein is based on the mathematical model in [8].

In the rest of this paper, a simplified model valid for a motion in the vertical plane is introduced without considered disturbances. A suitable choice of the output is proven to be locally minimum phase. The system is then input-output linearized. Some simulations are presented to illustrate the

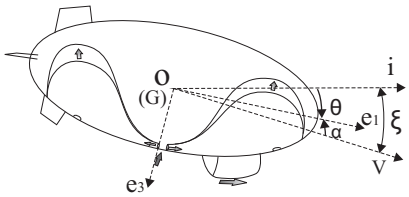

Fig. 3. Descent of Buoyancy-Driven Airship

controller's performance.

The rest of the paper is organized as follows. In section II, the mathematical model of the buoyancy-driven airship presented in [8] is recalled. The model is further simplified based on some principles in section III. In section IV, it is proved that the simplified model is minimum phase with the selected output and a nonlinear controller is designed to linearize it. The impact of the pole placement for closed loop stabilisation is illustrated by simulation results.

II. Preliminaries

The following complete mathematical model of the 6DOF buoyancy-driven airship has been derived in [8].

$$\begin{pmatrix} \dot{R} \\ \dot{\boldsymbol{b}} \\ \dot{\boldsymbol{\Omega}} \\ \dot{\boldsymbol{V}} \\ \dot{\boldsymbol{r}}_{\boldsymbol{p}} \\ \dot{\boldsymbol{B}}_{\boldsymbol{p}} \\ \dot{m}_b \end{pmatrix} = \begin{pmatrix} R\hat{\boldsymbol{\Omega}} \\ R\boldsymbol{V} \\ \boldsymbol{J_s^{-1}}\bar{\boldsymbol{M}} \\ \boldsymbol{m_s^{-1}}\bar{\boldsymbol{F}} \\ \frac{1}{\bar{m}}\boldsymbol{B_p} - \boldsymbol{V} - \boldsymbol{\Omega}\times\boldsymbol{r_p} \\ \bar{m}g(R^T\boldsymbol{k}) + \boldsymbol{B_p}\times\boldsymbol{\Omega} + \boldsymbol{u} \\ u_4 \end{pmatrix} \quad (1)$$

where, $\bar{\boldsymbol{M}}$ is a moment matrix, and $\bar{\boldsymbol{F}}$ is a force matrix. The values of $\bar{\boldsymbol{M}}$ and $\bar{\boldsymbol{F}}$ are as follows,

$$\begin{aligned} \bar{\boldsymbol{M}} &= (\boldsymbol{J_s\Omega} + \hat{\boldsymbol{r}}_{\boldsymbol{p}}\boldsymbol{B_p})\times\boldsymbol{\Omega} + \boldsymbol{m_s V}\times\boldsymbol{V} \\ &\quad + R^T\boldsymbol{M} - \hat{\boldsymbol{r}}_{\boldsymbol{p}}R^T\boldsymbol{F_p} \\ \bar{\boldsymbol{F}} &= (\boldsymbol{m_s V} + \boldsymbol{B_p})\times\boldsymbol{\Omega} + R^T\boldsymbol{F} - R^T\boldsymbol{F_p} \end{aligned}$$

The state variables and the rest of the parameters are explained in Table I.

To control the motion of the airship, we start from the most simple case, when the airship only flis in the vertical plane $i-k$, see Figure 1. In this case the equations are

$$\begin{aligned} \dot{v}_1 &= \frac{1}{m_1}(-m_3v_3\Omega_2 + (\bar{m}-m_0)\,g\sin\theta \\ &\quad + Z_a\sin\alpha - X_a\cos\alpha - u_1) && (2) \\ \dot{v}_3 &= \frac{1}{m_3}(m_1v_1\Omega_2 + (\bar{m}+m_0)\,g\sin\theta \\ &\quad - Z_a\cos\alpha - X_a\sin\alpha - u_3) && (3) \\ \dot{\Omega}_2 &= \frac{1}{J_2}((m_3-m_1)\,v_1v_3 + M_a + r_{p1}u_3 \\ &\quad - r_{p3}u_1) && (4) \\ \dot{\theta} &= \Omega_2 && (5) \\ \dot{r}_{p1} &= \frac{1}{\bar{m}}B_{p1} - v_1 - r_{p3}\Omega_2 && (6) \\ \dot{r}_{p3} &= \frac{1}{\bar{m}}B_{p3} - v_3 - r_{p1}\Omega_2 && (7) \\ \dot{B}_{p1} &= -B_{p3}\Omega_2 - \bar{m}g\sin\theta + u_1 && (8) \\ \dot{B}_{p3} &= B_{p1}\Omega_2 + \bar{m}g\cos\theta + u_3 && (9) \\ \dot{m}_b &= u_4 && (10) \\ \dot{x} &= v_1\cos\theta + v_3\sin\theta && (11) \\ \dot{z} &= -v_1\sin\theta + v_3\cos\theta && (12) \end{aligned}$$

TABLE I
NOMENCLATURE

Notation	Description
α	attack angle, $\alpha = \arctan(v_3/v_1)$
θ	pitch angle
$\boldsymbol{\Omega}$	$\boldsymbol{\Omega} = (\Omega_1, \Omega_2, \Omega_3)^T$, angular velocity in the body frame
$\boldsymbol{b}$	the position of the airship in the inertial frame
$\boldsymbol{B_p}$	$\boldsymbol{B_p} = (B_{p1}, B_{p2}, B_{p3})^T$, the momentums of the ballast
$\boldsymbol{F}$	the total external forces on the airship
$\boldsymbol{F_p}$	total external forces on the ballast
$\boldsymbol{J_s}$	the moment of inertia of the airship
J_2	sum of the moment of inertia and added inertia about e_2
$\boldsymbol{k}$	a unit vector along the direction of the gravity
m_b	the mass of the ballonet
m_s	the stationary mass of the airship
$\bar{m}$	the mass of ballast
m_1, m_3	sum of body and added mass along e_1, e_3 axis
m_0	the net buoyancy of the airship
$\boldsymbol{M}$	the total external moments on the airship
M_a	aerodynamic pitch moment
$\boldsymbol{r_p}$	$\boldsymbol{r_p} = (r_{p1}, r_{p2}, r_{p3})^T$, the position of the ballast
R	rotation matrix
$\boldsymbol{u}$	$\boldsymbol{u} = (u_1, u_2, u_3)^T$, vector of control inputs
$\tilde{\boldsymbol{u}}$	$\tilde{\boldsymbol{u}} = (\tilde{u}_1, \tilde{u}_2, \tilde{u}_3)^T$, transformed vector of control inputs
u_4	the control input of the mass of the ballast
$\boldsymbol{V}$	$\boldsymbol{V} = (v_1, v_2, v_3)^T$, velocity along e_1, e_2, e_3 axes
w_1	designed input for I/O linearization
λ_1, λ_0	parameters of the feedback controller
$\boldsymbol{x}$	$\boldsymbol{x} = (\theta, \Omega_2, v_1, v_3, r_{p1}, B_{p1})^T$, system states
$\boldsymbol{x_e}$	$\boldsymbol{x_e} = (\theta_e, \Omega_{2_e}, v_{1_e}, v_{3_e}, r_{p1_e}, B_{p1_e})^T$, equilibrium
X_a	drag, aerodynamic force
Z_a	lift, aerodynamic force

III. Simplified model

In the mathematical model (2)-(12), the position of the ballast is represented by r_{p1} and r_{p3}, which are unbounded in the system. That means the ballast can freely move in the vertical plane. But the ballast's movement along e_3 axis has little contribution to the control of the attitude and velocity of the airship, and the movement of the ballast along this direction also leads to unnecessary complexity and unstability to the system, because the airship should have "bottom-heaviness". The ballast's movement on the negative direction of e_3 axis contributes to the unstable "top-heaviness" [7]. So it is assumed that the ballast is fixed at a constant height. That means a fixed value of r_{p3} and to cancel u_3 and B_{p3}. A fixed height of the ballast also makes the actuators more simple and easy to realize. Under these cosiderations we may proceed to simplify the math model.

First, we simplify (8) and (9) as follows,

$$\begin{aligned} \dot{B}_{p1} &= \tilde{u}_1 \\ \dot{B}_{p3} &= \tilde{u}_3 \end{aligned}$$

where, $\tilde{u}_1$ and $\tilde{u}_3$ denote the total external forces on the ballast, which is different from u_1 and u_3 that only denote the external forces from the body of airship.

With fixed r_{p3}, the right hand side of equation (7) is equal to zero. So $B_{p3} = \bar{m}(v_3 - r_{p1}\Omega_2)$ and $\tilde{u}_3 = \dot{B}_{p3} = \bar{m}(\dot{v}_3 - \dot{r}_{p1}\Omega_2 - r_{p1}\dot{\Omega}_2)$. Combining with equations (4), (2) and (6), the new functions of $\dot{\Omega}_2$ and $\dot{v}_3$ can be derived.

To further simplify the model, it is assumed that during the routine fly, we just adjust the position of the ballast to cope

with general disturbances. This assumption is reasonable, because compared with changing the mass of the ballonets, it is easy and energetically economic to change the position of the ballast, and in this paper, we just focus on the stabilization of airship during straight line cruise. So it is unnecessary to change the mass of the ballonets which is denoted by m_b.

x and z are the position of the airship in the vertical plane with respect to the inertial frame. Since our control objective will be tracking the attitude angle ξ, and not path following. equations (11) and (12) can be ignored.

Integrating the above suggestions to simplify the model (2)-(12), it reduces to six states $\boldsymbol{x} = (\theta, \Omega_2, v_1, v_3, r_{p1}, B_{p1})^T$ and one control input $\tilde{u}_1$:

$$\begin{aligned}
\dot{\theta} &= \Omega_2 && (13)\\
\dot{\Omega}_2 &= T_1 H_1 + T_2 H_2 && (14)\\
\dot{v}_1 &= H_3/m_1 && (15)\\
\dot{v}_3 &= T_2 H_1 + T_3 H_2 && (16)\\
\dot{r}_{p1} &= B_{p1}/\bar{m} - v_1 - r_{p3}\Omega_2 && (17)\\
\dot{B}_{p1} &= \tilde{u}_1 && (18)
\end{aligned}$$

where

$$\begin{aligned}
T_1 &= \frac{m_3 + \bar{m}}{J_2\,(m_3 + \bar{m}) + \bar{m} m_3 r_{p1}^2}\\
T_2 &= \frac{\bar{m} r_{p1}}{J_2\,(m_3 + \bar{m}) + \bar{m} m_3 r_{p1}^2}\\
T_3 &= \frac{J_2 + \bar{m} r_{p1}^2}{J_2\,(m_3 + \bar{m}) + \bar{m} m_3 r_{p1}^2}
\end{aligned}$$

$$\begin{aligned}
H_1 &= (m_3 - m_1)\, v_1 v_3 - \bar{m} g\,(r_{p1}\cos\theta + r_{p3}\sin\theta)\\
&\quad - (r_{p1} B_{p1} + r_{p3}\bar{m}\,(v_3 - r_{p1}\Omega_2))\,\Omega_2 + M_a\\
&\quad - r_{p3}\tilde{u}_1 + \bar{m} r_{p1}\Omega_2\,(v_1 + r_{p3}\Omega_2) - r_{p1}\Omega_2 B_{p1}\\
H_2 &= m_1 v_1 \Omega_2 + B_{p1}\Omega_2 + m_0 g\cos\theta - Z_a\cos\alpha\\
&\quad - X_a\sin\alpha - \bar{m}\Omega_2(v_1 - r_{p3}\Omega_2) + B_{p1}\Omega_2\\
H_3 &= -m_3 v_3 \Omega_2 - \bar{m}(v_3 - r_{p1}\Omega_2)\Omega_2 - m_0 g\sin\theta\\
&\quad + Z_a\sin\alpha - X_a\cos\alpha - \tilde{u}_1
\end{aligned}$$

IV. Nonlinear controller

In [8], a linear controller was derived using a LQR optimal method. This linear controller displays good control performances, but valid only in a small neighborhood around the equilibrium. In this section, a nonlinear controller based on I/O linearization is designed for the system whose internal stability is proved.

A. Stability of zero dynamics

Define $\boldsymbol{x} = (\theta, \Omega_2, v_1, v_3, r_{p1}, B_{p1})^T$. Then equations (13)-(18) are rewritten in the following form,

$$\dot{\boldsymbol{x}} = \boldsymbol{f}(\boldsymbol{x}) + \boldsymbol{g}(\boldsymbol{x})\tilde{u}_1\ .$$

Consider the output of the system $y = x$, that is the six states. Both variables θ and r_{p1} have relative degree 2 [10]. However, it is easy to check that considering the output r_{p1} yields a non minimum phase systems and thus, input-output linearization can not be applied; whereas the output function θ defines a minimum phase system.

The unforced system has an equilibrium $\boldsymbol{x_e}$ which can obtained from solving $\boldsymbol{f(x_e)} = 0$. For the chosen parameter, $\boldsymbol{x_e} = (\theta_e, \Omega_{2_e}, v_{1_e}, v_{3_e}, r_{p1_e}, B_{p1_e})^T = (0.44, 0, 9.97, -0.8, -1, 299)^T$. The linear approximation around this point is

$$\dot{\boldsymbol{x}} = \boldsymbol{A}\boldsymbol{x} + \boldsymbol{B}\tilde{u}_1 \qquad (19)$$

where,

$$A = \begin{pmatrix}
0 & 1 & 0 & 0 & 0 & 0\\
-0.08 & 0.01 & -0.0004 & 0.004 & -0.03 & 0\\
0.57 & 0.93 & -0.063 & -0.17 & 0 & 0\\
0.24 & 9.13 & 0.05 & -0.62 & 0.002 & 0\\
0 & -2 & -1 & 0 & 0 & 0.03\\
0 & 0 & 0 & 0 & 0 & 0
\end{pmatrix}$$

$$B = \begin{pmatrix}
0\\ -0.0002\\ -0.002\\ 0.00001\\ 0\\ 1
\end{pmatrix}$$

and whose transfer function is easily computed as

$$TF_1 = \frac{-0.02s^4 - 0.02s^3 - 0.1s^2 - 0.08s - 0.005}{100s^6 + 67s^5 + 1.9s^4 - 2.3s^3 - 5s^2 - s}$$

for $y = \theta$, and

$$TF_2 = \frac{3.6s^4 + 2.4s^3 + 0.3s^2 + 0.2s + 0.01}{100s^6 + 67s^5 + 1.9s^4 - 2.3s^3 - 5s^2 - s}$$

for $y = r_{p1}$.

The four zeros of TF_1 have negative real part, whereas some of TF_2 have positive real part and thus are unstable.

Since the linear approximation of the system (13)-(18) with the output $y = \theta$ has stable transmission zeros, the nonlinear system has locally stable zero dynamics and thus the system is minimum phase [9].

B. I/O linearization of θ

Since the relative degree of the output $y = \theta$ is 2, we propose the following desired error equation

$$\ddot{e} + \lambda_1\dot{e} + \lambda_0 e = w_1$$

where $e = y - \theta_e$, θ_e is the desired value for θ, and w_1 denotes a new control input. Equivalently,

$$\ddot{\theta} + \lambda_1\dot{\theta} + \lambda_0(\theta - \theta_e) = w_1 \qquad (20)$$

λ_1 and λ_0 assign the poles of the error dynamics. Substituting (13) and (14) into (20), the equation can be solved and the control $\tilde{u}_1$ derived, as follows,

$$\tilde{u}_1 = T_4(H_4 - w_1 + \lambda_1\Omega_2 + \lambda_0(\theta - \theta_e)) \qquad (21)$$

where,

$$\begin{aligned} T_4 &= \frac{J_2 m_3 + J_2 \bar{m} + \bar{m} r_{p1}^2 m_3}{r_{p3}(m_3 + \bar{m})} \\ H_4 &= T_1(H_1 + r_{p3}\tilde{u}_1) + T_2 H_2 \end{aligned}$$

Equation (21) is the nonlinear feedback controller of the system. Let $w_1 = 0$, and substituting (21) into (13)-(18), the closed loop system will be derived.

The choice of the values of λ_1 and λ_0 not only has a direct impact on the motion of θ and Ω_2, but also a significant one on the states v_1, v_3, r_{p1} and B_{p1}. The impact on the θ and Ω_2 are easy to analyze, but the transient response of v_1, v_3, r_{p1} and B_{p1} remains unclear due to the nonlinear equations. By trying different values of λ_1 and λ_0, different performances of the controller are presented.

C. Simulation results

The airship is desired to fly with angle ξ_e and velocity V_e, see Figure 1 and 4. In this paper, we only consider the control during the upward and downward phase, and do not consider the transfer between these two phases. The conditions in the downward phase are the same as the upward phase with only reversed values of some states and parameters.

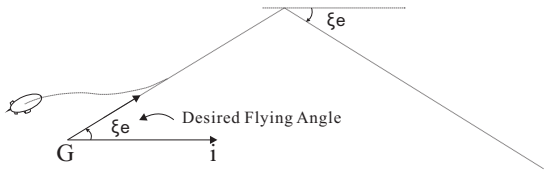

Fig. 4. Flying Sketch

The parameters used in this project are taken from [8]. The value of the states on the equilibrium $\boldsymbol{x_e}$ are presented in the section IV.A of this paper.

When deciding the values of λ_1 and λ_0, there is a tradeoff between the performance of θ and Ω_2 with respect to the one of states v_1, v_3, r_{p1} and B_{p1}, and thus they must be carefully chosen. To this end, we will present three different sets of λ_1 and λ_0. All of these simulations are under initial errors $\Delta\theta = +5^\circ$ and $\Delta v_1 = +2\ m/s$.

To compare the results of different parameters, the poles under different sets of parameters should have the same negative real part, so θ stabilizes in a similar period, see Figure 5.

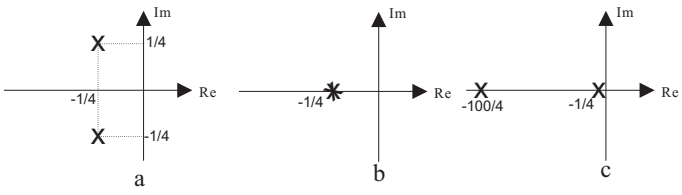

Fig. 5. Three Different Assignments of Poles

First strategy: two complex poles

The poles are chosen to be of the form $s = -a(1 \pm i)$. For the reported simulation, $a = 1/4$, so $\lambda_1 = 1/2$ and $\lambda_0 = 1/8$, see Figure 5.a. This is called Controller No. 1.

Second strategy: a double real pole

Both poles are placed at $-a$, with $a = -1/4$, see Figure 5.b. So the controller No. 2 is with $\lambda_1 = 0.5$ and $\lambda_0 = 0.0625$.

Third strategy: a dominant real pole

The last considered strategy is to obtain a first-order like response by placing a dominant pole. Controller No. 3 has two different negative real poles. One pole close to the imaginary axis, another is far away from the imaginary axis. Let $s_1 = -\frac{1}{4}$, $s_2 = -\frac{100}{4}$, see Figure 5.c, so $\lambda_1 = 25.25$ and $\lambda_0 = 6.25$.

The dynamics of θ under these controllers are presented in Figure 6. Figure 7 and 8 are the dynamics of v_1 and v_3 with the controller No. 3. To different controllers, the mainly difference of dynamics of v_1 and v_3 is the final values. Figure 9 to 11 are the dynamics of r_{p1} which presents the movement of the ballast.

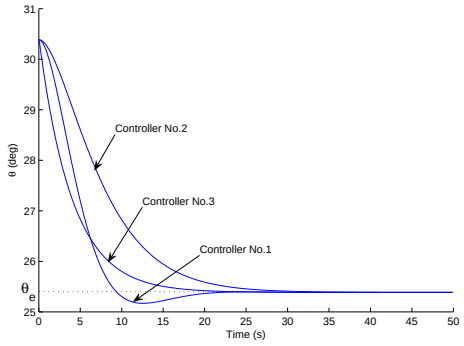

Fig. 6. Comparison of Dynamics of θ

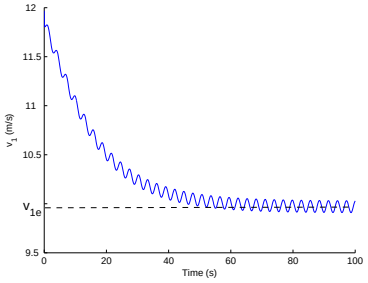

Fig. 7. Dynamics of v_1

D. Analysis of the Simulation Result

Generally, from the simulation results, the system is stable under certain initial errors with these controllers, but the differences between three controllers are significant.

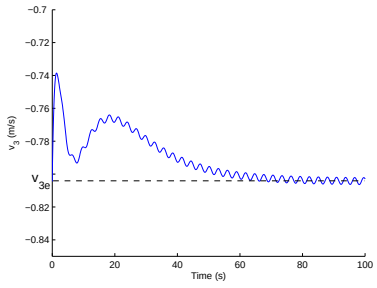

Fig. 8. Dynamics of v_3

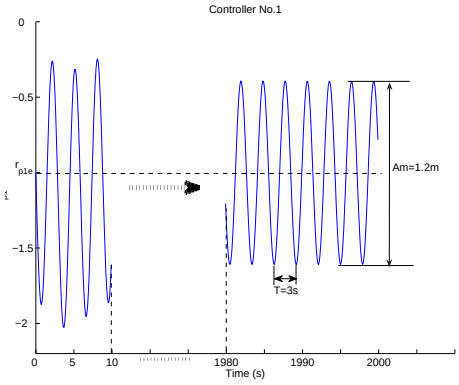

Fig. 9. Dynamics of r_{p1} with Controller No.1

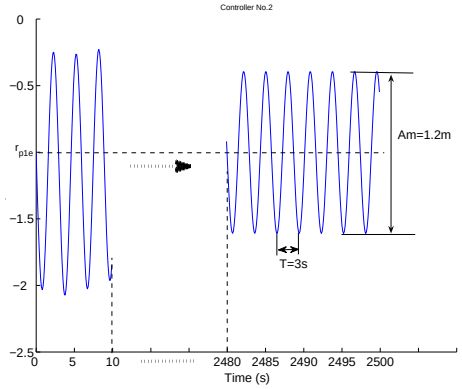

Fig. 10. Dynamics of r_{p1} with Controller No.2

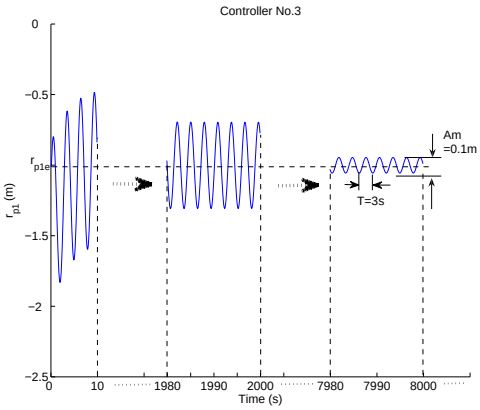

Fig. 11. Dynamics of r_{p1} with Controller No.3

In detail, from Figure 6, the three controllers have similar stationarity and rapidity, which is due to the same negative real parts, see Figure 5. Both θ and Ω_2 stabilize at the equilibrium point quickly, which is the goal of these feedback controllers.

With respect to v_1 and v_3, they have small periodic oscillations under three conditions, but the final amplitudes are different. With controller No. 1 and No.2, the final amplitudes are the same, which is $0.14\ m/s$ for v_1, and v_3 is small enough to be ignored. The controller No. 3 has much better performance. To v_1, the final amplitude is $0.01\ m/s$, and v_3 attenuates to v_{3_e} quickly.

From Figure 9 to 11, we can more clearly find that controller No. 3 is better than the two others. The amplitude of r_{p1} under controller No. 3 continually declines with the time, but it is constant under controllers No. 1 and No. 2.

These controllers are also sensitive to the initial errors as with the LQR controller in [8], since large initial errors will lead to unstability. However, the bound is much more broad.

V. Conclusions and Future Work

A. Conclusions

With these controllers, v_1, v_3, r_{p3} and B_{p1} have periodic oscillations, with a period approximately of 3 s, which is acceptable for the system. These oscillations are associated to the complex zeros of the linear approximation close to the imaginary axis. Here, two of the zeros of TF_1 are $-2.85 \times 10^{-4} \pm 2.16i$.

These nonlinear controllers are better than linear LQR controllers for autonomous buoyancy-driven objects, since the nonlinear controllers have larger stable domain of initial conditions than the linear LQR one, which can be illustrated by simulations. When the initial error of v_1 is larger than $+4.5\ m/s$, the linear controller no more ensures stability and the airship crashes down [8]. But these nonlinear controllers also ensure stability in a certain domain, and large initial errors lead to larger oscillations.

B. Future Work

In this paper, we presented a nonlinear controller based on input-output linearization, using an output with relative degree 2. An open research line is the search of outputs with maximal relative degree to obtain the smallest internal dynamics. Also the behavior of the internal dynamics suggests the existence of stable limit cycles, which produces a continuous change of speed and orientation. Further research is required to eliminate these limit cycles, or maximally reduce their amplitude at least.

References

[1] T. C. Tozer and D. Grace, *High-altitude platforms for wireless communications*, IEE Electron. Commun. Eng. J., vol. 13, no. 3, pp. 127137, Jun. 2001.

[2] Naval Research Advisory Committee, *Lighter Than Air Systems for Future Naval Missions* Briefing: Flag Officers and Senior Executive Service, The Pentagon Auditorium, Washington D.C., October, 2005.
[3] Gomes V B, Ramos J G. *Airship dynamic modeling for autonomous operation*, IEEE Int. Conf. on Robotics and Automation, 1998. pp. 3462-3467.
[4] J. Ouyang, *Research on modeling and control of an unmanned airship*, Dissertation for the Doctor Degree, Shanghai Jiaotong University, 2003.
[5] R. Purandare, *A buoyancy-propelled airship*, Dissertation for the Doctor Degree of Philosophy, New Mexico State University, 2007
[6] N. Leonard and J. Graver, *Model-based feedback control of autonomous underwater gliders*, IEEE Journal of Oceanic Engineering, Vol. 26, No. 4, October 2001.
[7] N. Leonard, *Stability of a bottom-heavy underwater vehicle*, Automatica, Vol. 33, No. 3, pp. 331-346, 1997
[8] X. WU, C.H. Moog and Y. Hu, *Modelling and linear control of a buoyancy-driven airship*, submited to ASCC09
[9] G. Conte, C. H. Moog and A.M. Perdon, *Algebraic Methods for nonlinear control systems-theory and applications*, Chapter 3 and 9, 2nd Edition, Springer, 2006
[10] A. Isidori, *Nonlinear control systems: an introduction*, Chapter 4, Springer, 1999